

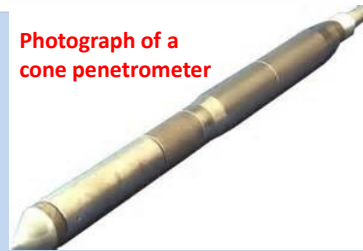
2.15 CONE PENETRATION TEST

L6/P1

The cone penetration test (CPT), originally known as the Dutch cone penetration test, is a versatile sounding method that can be used to determine the materials in a soil profile and estimate their engineering properties. This test is also called the static penetration test, and no boreholes are necessary to perform it. In the original version, a 60° cone with a base area of 10 cm² was pushed into the ground at a steady rate of about 20 mm/sec, and the resistance to penetration (called the point resistance) was measured.

The cone penetrometers in use at present measure (a) the cone resistance (q_c) to penetration developed by the cone, which is equal to the vertical force applied to the cone divided by its horizontally projected area, and (b) the frictional resistance (f_c), which is the resistance measured by a sleeve located above the cone with the local soil surrounding it. The frictional resistance is equal to the vertical force applied to the sleeve divided by its surface area — actually, the sum of friction and adhesion.

Photograph of a
cone penetrometer



1

Two types:

- (a) Mechanical friction cone penetrometer
- (b) Electric friction cone penetrometer

Photograph of a
cone penetrometer



q_c = Cone resistance; f_c = Side friction

q_c = Total force acting on the cone divided by its projected area (10 cm²)

f_c = Total frictional force acting on the friction sleeve divided by its surface area (150 cm²)

Usually the friction ratio, R_f is calculated from q_c and f_c . $R_f = f_c / q_c$

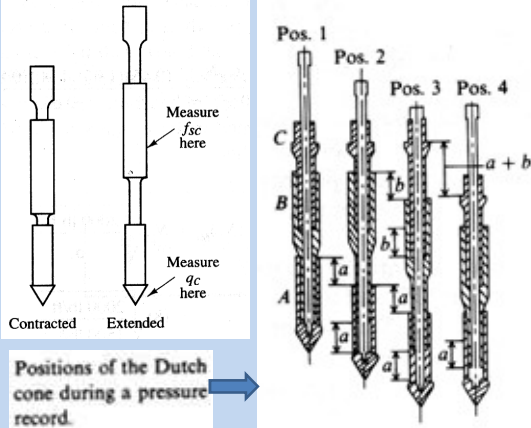
There is another type of cone equipped with pore pressure transducer that measures the excess pore water pressure that develop while conducting the test.

These are known as piezocone and the enhanced procedure is known as a CPTU test.

This particularly useful in saturated clays.

2

a. *Mechanical friction-cone penetrometer* (Figure 2.28). In this case the penetrometer tip is connected to an inner set of rods. The tip is first advanced about 40 mm giving the cone resistance. With further thrusting, the tip engages the friction sleeve. As the inner rod advances, the rod force is equal to the sum of the vertical force on the cone and sleeve. Subtracting the force on the cone gives the side resistance.

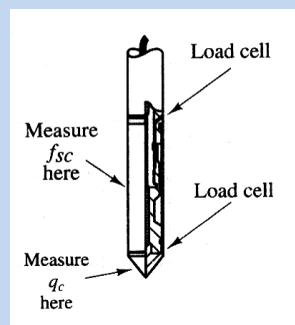


Mechanical cone is advanced in stages and measures q_c and q_s at intervals of about 20cm, whereas electric cone (fitted with strain-gauge) measure these quantities continuously

- Pos.1: Cone is seated
- Pos.2: Cone is pushed to measure q_c
- Pos.3: Both Cone & Friction sleeve are pushed to measure $q_t = q_c + q_s$
- Pos.4: Friction sleeve is pushed to measure q_s

3

b. *Electric friction-cone penetrometer* (Figure 2.29). In this case the tip is attached to a string of steel rods. The tip is pushed into the ground at the rate of 20 mm/sec. Wires from the transducers are threaded through the center of the rods and continuously give the cone and side resistances.



Electric cone (fitted with strain-gauge) measure q_c and q_s continuously with depth

4

L6/P3

Photographs of CPT equipments (source internet)



<http://www.griffithsdrilling.co.nz/services/conepenetrationtest.aspx>



http://www.brighthubengineering.com/geotechnical-engineering/48648-geotechnical-examination-and-analysis/#imgn_1



<http://brs.upd.edu.ph/featured/>



<http://earthquake.usgs.gov/research/cpt/>



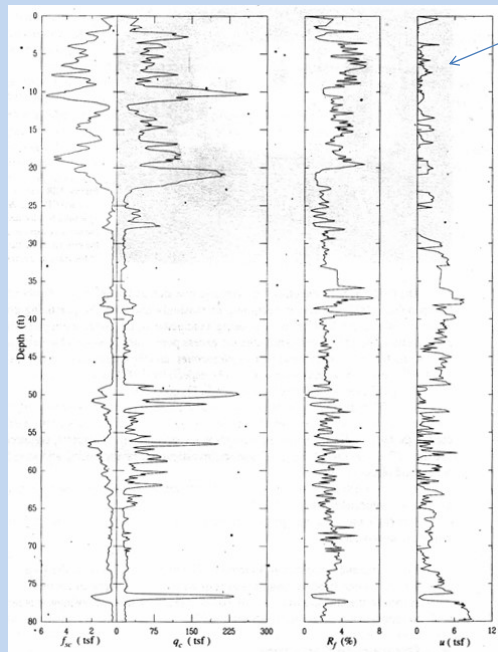
<http://geotechnicaldesign.info/fotobank/cone-penetration-test.html>

Equipments vary in thrust capacity and thus maximum depth of exploration

5

CPT TEST RESULTS

L6/P6



Additional information from CPTU (pore water pressure vs. depth)

(Geotechnical Engineering, principles and Practice/Coduto/p.78)

6

L6/P7

Advantages of CPT

- CPT is a useful means to determine the soil profile. Since it retrieves data continuously with depth (with electric cone) or at very close interval (with mechanical cone), CPT can detect thin layers in stratigraphy. Sometimes use of CPT in the first phase facilitate better specification for boring and sampling in the second phase.
- It is also less prone to error due to automated operation of the equipment and electronic data recording.

Disadvantages of CPT

- No soil sample is recovered. So no opportunity to inspect the soils.
- The test is unreliable or unusable in soils with significant gravel content.
- Although the cost per foot of penetration is less than that for borings, it is necessary to mobilize a special rig to perform the CPT. CPT at a certain site may not be possible from the point of equipment mobilization.

7

CPT correlations

L6/P8

Cone resistance, $q_c \sim$ Relative Density, D_r

Lancellotta (1983) and Jamiolkowski et al. (1985) showed that the relative density of normally consolidated sand, D_r , and q_c can be correlated as

$$D_r(\%) = A + B \log_{10} \left(\frac{q_c}{\sqrt{\sigma'_v}} \right) \quad (2.25)$$

where $A, B =$ constants
 $\sigma'_v =$ vertical effective stress

The values of A and B are

A	B	Unit of q_c and σ'_v
-98	66	metric ton/m ²

8

L6/P9

Cone resistance, $q_c \sim$ Relative Density, D_r contd.

Figure 2.31 shows the correlations obtained for several sands. Baldi et al. (1982), and Robertson and Campanella (1983) also recommended an empirical relationship between vertical effective stress (σ'_v), relative density (D_r), and q_c for normally consolidated sand. This is shown in Figure 2.32.

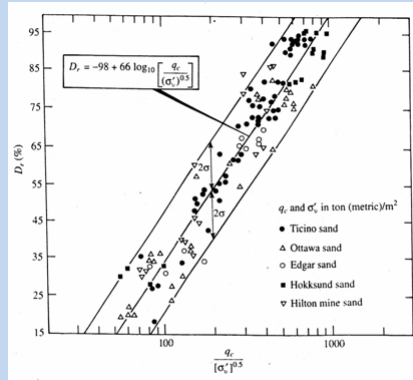


FIGURE 2.31 Relationship between D_r and q_c (based on Lancellotta, 1983, and Jamioilkowski et al., 1985)

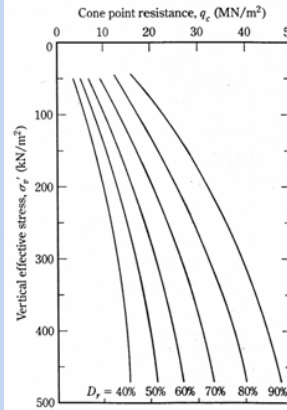


FIGURE 2.32 Variation of q_c , σ'_v , and D_r for normally consolidated quartz sand (based on Baldi et al., 1982, and Robertson and Campanella, 1983)

9

Cone resistance, $q_c \sim$ Angle of internal friction, ϕ

L6/P10

Figure 2.33 shows a correlation between σ'_v , q_c , and the peak friction angle ϕ for normally consolidated quartz sand. This correlation can be expressed as (Kulhawy and Mayne, 1990)

$$\phi = \tan^{-1} \left[0.1 + 0.38 \log \left(\frac{q_c}{\sigma'_v} \right) \right] \quad (2.26)$$

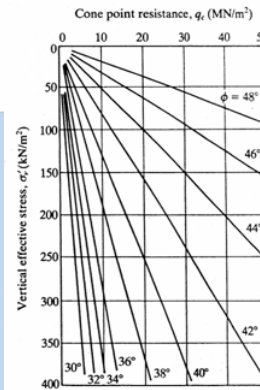


FIGURE 2.33 Variation of q_c with σ'_v and ϕ in normally consolidated quartz sand (after Robertson and Campanella, 1983)

10

Cone resistance, $q_c \sim$ Friction ratio, F_f

Robertson and Campanella (1983) also provided a general correlation between q_c , friction ratio F_f , and the type of soil encountered in the field (Figure 2.34). Figure 2.35 shows the general range of q_c/N_f for various types of soil.

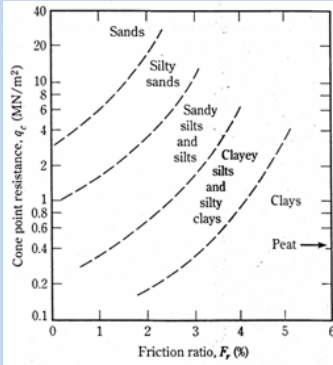


FIGURE 2.34 Robertson and Campanella's correlation (1983) between q_c , F_f , and the soil type

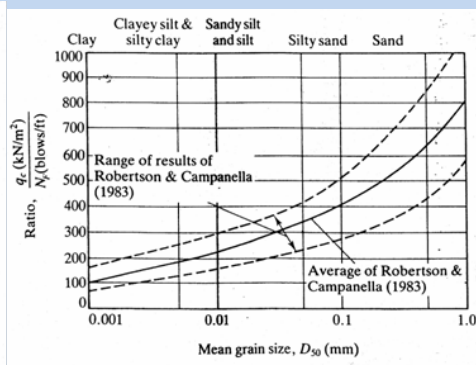


FIGURE 2.35 General range of variation of q_c/N_f for various types of soil (after Robertson and Campanella, 1983)

According to Mayne and Kemper (1988), in clayey soil the undrained cohesion c_u , preconsolidation pressure p_c , and the overconsolidation ratio can be correlated as

$$\left(\frac{c_u}{\sigma'_v}\right) = \left(\frac{q_c - \sigma_v}{\sigma'_v}\right) \frac{1}{N_K} \quad (2.27) \quad \text{or} \quad c_u = \frac{q_c - \sigma_v}{N_K} \quad (2.27a)$$

where N_K = bearing capacity factor ($N_K = 15$ for electric cone and $N_K = 20$ for mechanical cone)
 σ_v = total vertical stress
 σ'_v = effective vertical stress

Consistent units of c_u , σ_v , σ'_v , and q_c should be used with Eq. (2.27):

$$p_c = 0.243(q_c)^{0.96} \quad (2.28) \quad \text{and} \quad OCR = 0.37 \left(\frac{q_c - \sigma_v}{\sigma'_v}\right)^{1.01} \quad (2.29)$$

\uparrow \uparrow
 MN/m² MN/m²

where σ_v and σ'_v = total and effective stress, respectively

L6/P13

PRESSUREMETER TEST (PMT)

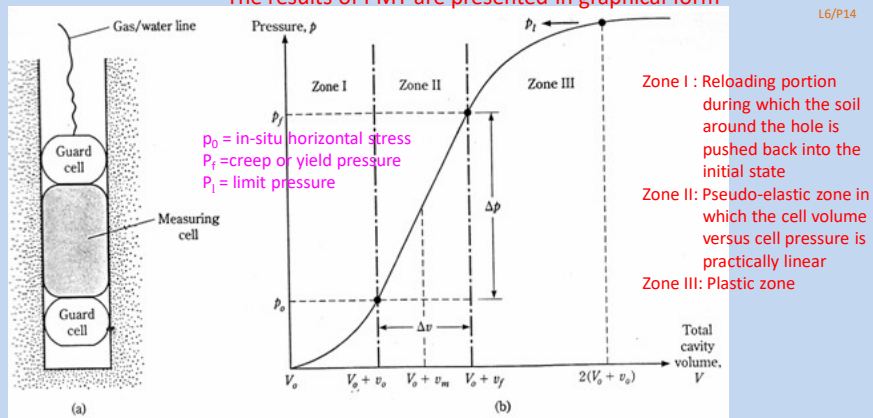
The pressuremeter test is an *in situ* test conducted in a borehole. It was originally developed by Menard (1956) to measure the strength and deformability of soil. It has also been adopted by ASTM as Test Designation 4719. The Menard-type PMT essentially consists of a probe with three cells. The top and bottom ones are *guard cells* and the middle one is the *measuring cell*, as shown schematically in Figure 2.36a. The test is conducted in a pre-bored hole. The pre-bored hole should have a diameter that is between 1.03 to 1.2 times the nominal diameter of the probe. The probe that is most commonly used has a diameter of 58 mm and a length of 420 mm. The probe cells can be expanded either by liquid or gas. The guard cells are expanded to reduce the end-condition effect on the measuring cell. The measuring cell has a volume (V_0) of 535 cm³. Following are the dimensions for the probe diameter and the diameter of the borehole as recommended by ASTM:

Probe diameter (mm)	Borehole diameter	
	Nominal (mm)	Maximum (mm)
44	45	53
58	60	70
74	76	89

In order to overcome the difficulty of preparing the borehole to the proper size self-boring pressuremeters (SBPMT) have been developed

13

The results of PMT are presented in graphical form



L6/P14

FIGURE 2.36 (a) Pressuremeter; (b) plot of pressure versus total cavity volume

In order to conduct a test, the measuring cell volume, V_0 , is measured and the probe is inserted into the borehole. Pressure is applied in increments and the volumatic expansion of the cell is measured. This is continued until the soil fails or until the pressure limit of the device is reached. The soil is considered to have failed when the total volume of the expanded cavity (V) is about twice the volume of the original cavity. After the completion of the test, the probe is deflated and advanced for test at another depth.

14

L6/P15

The results of the pressuremeter test is expressed in a graphical form of pressure versus volume as shown in Figure 2.36b. In this figure, Zone I represents the reloading portion during which the soil around the borehole is pushed back into the initial state (that is, the state it was in before drilling). The pressure, p_o , represents the *in situ* total horizontal stress. Zone II represents a pseudo-elastic zone in which the cell volume versus cell pressure is practically linear. The pressure, p_f , represents the creep, or yield, pressure. The zone marked III is the plastic zone. The pressure, p_l , represents the limit pressure.

The pressuremeter modulus, E_p , of the soil is determined using the theory of expansion of an infinitely thick cylinder. Thus

$$E_p = 2(1 + \mu)(V_o + v_m) \left(\frac{\Delta p}{\Delta v} \right) \quad (2.30)$$

where $v_m = \frac{v_o + v_f}{2}$

$$\Delta p = p_f - p_o$$

$$\Delta v = v_f - v_o$$

$$\mu = \text{Poisson's ratio (which may be assumed to be 0.33)}$$

15

L6/P16

Correlations between various soil parameters and the results obtained from the pressuremeter tests have been developed by various investigators. Kulhawy and Mayne (1990) proposed that

$$p_c = 0.45p_l \quad (2.31)$$

where p_c = preconsolidation pressure

Based on the cavity expansion theory, Baguelin et al. (1978) proposed that

$$c_u = \frac{(p_l - p_o)}{N_p} \quad (2.32)$$

where c_u = undrained shear strength of a clay

$$N_p = 1 + \ln \left(\frac{E_p}{3c_u} \right)$$

Typical values of N_p vary between 5 to 12, with an average of about 8.5. Ohya et al. (1982) (see also Kulhawy and Mayne, 1990) correlated E_p with field standard penetration numbers (N_F) for sand and clay as follows:

$$\text{Clay: } E_p (\text{kN/m}^2) = 1930N_F^{0.83} \quad (2.33)$$

$$\text{Sand: } E_p (\text{kN/m}^2) = 908N_F^{0.66} \quad (2.34)$$

16

Vane Shear Test

L6/P17

The *vane shear test* (ASTM D-2573) may be used during the drilling operation to determine the *in situ* undrained shear strength (c_u) of clay soils — particularly soft clays. The vane shear apparatus consists of four blades on the end of a rod, as shown in Figure 2.24. The height, H , of the vane is twice the diameter, D . The vane can be either rectangular or tapered (see Figure 2.24). The dimensions of vanes used in the field are given in Table 2.6. The vanes of the apparatus are pushed into the soil at the bottom of a borehole without disturbing the soil appreciably. Torque is applied at the top of the rod to rotate the vanes at a standard rate of 0.1°/sec. This rotation will induce failure in a soil of cylindrical shape surrounding the vanes. The maximum torque, T , applied to cause failure is measured. Note that

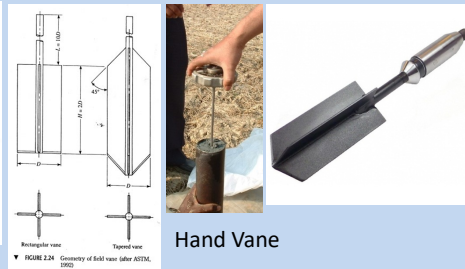
$$T = f(c_u, H, \text{ and } D) \quad (2.13)$$

or

$$c_u = \frac{T}{K} \quad (2.14)$$

where T is in N·m, and c_u is in kN/m²

K = a constant with a magnitude depending on the dimension and shape of the vane



Hand Vane

Field Vane

17

$$K = \left(\frac{\pi}{10^6}\right) \left(\frac{D^2 H}{2}\right) \left(1 + \frac{D}{3H}\right) \quad (2.15)$$

where D = diameter of vane in cm
 H = measured height of vane in cm

If $H/D = 2$, Eq. (2.15) yields

$$K = 366 \times 10^{-6} D^3 \quad (2.16)$$

↑
(cm)

In English units, if c_u and T in Eq. (2.14) are expressed in lb/ft² and lb-ft, respectively,

$$K = \left(\frac{\pi}{1728}\right) \left(\frac{D^2 H}{2}\right) \left(1 + \frac{D}{3H}\right) \quad (2.17)$$

If $H/D = 2$, Eq. (2.17) yields

$$K = 0.0021 D^3 \quad (2.18)$$

↑
(in.)

18

L6/P19

Advantages and Limitations of Field Vane Shear test

Field vane shear tests are moderately rapid and economical and are used extensively in field soil-exploration programs. The test gives good results in soft and medium-stiff clays, and it is also an excellent test to determine the properties of sensitive clays.

Sources of significant error in the field vane shear test are poor calibration of torque measurement and damaged vanes. Other errors may be introduced if the rate of vane rotation is not properly controlled.

For actual design purposes, the undrained shear strength values obtained from field vane shear tests [$c_u(\text{VST})$] are too high and it is recommended that they be corrected, or

$$c_{u(\text{corrected})} = \lambda c_{u(\text{VST})} \quad (2.19)$$

where λ = correction factor

Several correlations have been previously given for the correction factor, λ , and some are given in Table 2.7.

Undrained shear strength, pre-consolidation pressure and OCR can be determined using appropriate correlations.

19

L6/P20

For actual design purposes, the undrained shear strength values obtained from field vane shear tests [$c_u(\text{VST})$] are too high and it is recommended that they be corrected,

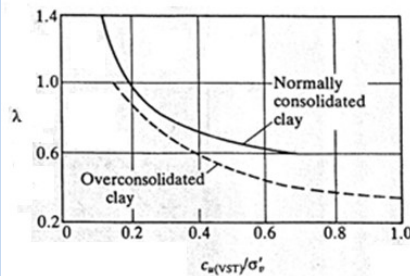
$$c_{u(\text{corrected})} = \lambda c_{u(\text{VST})} \quad (2.19)$$

where λ = correction factor

Several correlations for the correction factor, λ , are given in Table 2.7.

TABLE 2.7 Correlations for λ

Source	Correlation
Bjerrum (1972)	$\lambda = 1.7 - 0.54 \log(PI)$ $PI = \text{plasticity index (\%)}$
Morris and Williams (1994)	$\lambda = 1.18e^{-0.0607PI} + 0.57$ for $PI > 5$
Morris and Williams (1994)	$\lambda = 7.01e^{-0.0602LL} + 0.57$ $LL = \text{liquid limit (\%)}$
Aas et al. (1986)	



σ'_v = effective overburden pressure

20

Field vane shear strength ~ Pre-consolidation pressure

The field vane shear strength can also be correlated to preconsolidation pressure and the overconsolidation ratio of the clay. Using 343 data points, Mayne and Mitchell (1988) derived the following empirical relationship for estimation of the preconsolidation pressure of a natural clay deposit.

$$p_c = 7.04 [c_{v(\text{field})}]^{0.83} \quad (2.20)$$

where

p_c = preconsolidation pressure (kN/m²)
 $c_{v(\text{field})}$ = field vane shear strength (kN/m²)

Figure 2.25 shows the plot of the data points from which they derived the relationship.

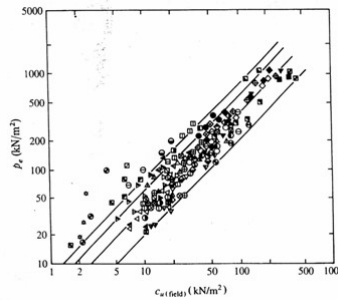


FIGURE 2.25 Variation of preconsolidation pressure with field vane shear strength (after Mayne and Mitchell, 1988)

They also showed that the overconsolidation ratio (OCR) can be correlated to $c_{v(\text{field})}$ as

$$OCR = \beta \frac{c_{v(\text{field})}}{\sigma'_v} \quad (2.21a)$$

where σ'_v = effective overburden pressure

$$\beta = 22 (PI)^{-0.68} \quad (2.21b)$$

where PI = plasticity index

Figure 2.26 shows the variation of β with plasticity index.

Other correlations for β presented in the literature are

Hansbo (1957)

$$\beta = \frac{222}{w(\%)} \quad (2.22)^{1/2}$$

Larsson (1980)

$$\beta = \frac{1}{0.08 + 0.0055(PI)} \quad (2.23)$$

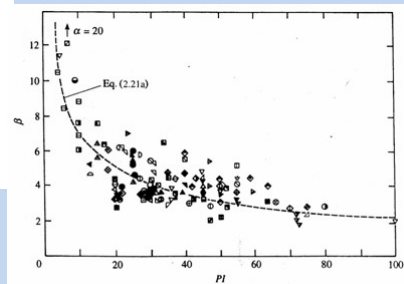


FIGURE 2.26 Variation of β with plasticity index (after Mayne and Mitchell, 1988)